Artificial Organs

Numerical Approach to Study the Behavior of an Artificial Ventricle: Fluid–Structure Interaction Followed by Fluid Dynamics With Moving Boundaries

*Giulia Luraghi, *†Wei Wu, ‡Hector De Castilla, *José Félix Rodriguez Matas, *Gabriele Dubini, ‡Pascal Dubuis, ‡Marc Grimmé and *Francesco Migliavacca

**Laboratory of Biological Structure Mechanics, Department of Chemistry, Materials and Chemical Engineering "Giulio Natta", Politecnico di Milano, Milan, Italy; †Department of Mechanical Engineering, University of Texas at San Antonio, San Antonio, TX, USA; and ‡Carmat, Vélizy-Villacoublay, France*

Abstract: Heart failure is a progressive and often fatal pathology among the main causes of death in the world. An implantable total artificial heart (TAH) is an alternative to heart transplantation. Blood damage quantification is imperative to assess the behavior of an artificial ventricle and is strictly related to the hemodynamics, which can be investigated through numerical simulations. The aim of this study is to develop a computational model that can accurately reproduce the hemodynamics inside the left pumping chamber of an existing TAH (Carmat-TAH) together with the displacement of the leaflets of the biological aortic and mitral valves and the displacement of the pericardium-made membrane. The proposed modeling workflow combines fluid–structure interaction (FSI) simulations based on a fixed grid method with computational fluid dynamics (CFD). In particular, the kinematics of the valves is accounted for by means of a dynamic mesh technique in the CFD. The comparison between FSI- and CFD-calculated velocity fields confirmed that the presence of the valves in the CFD model is essential for realistically mimicking blood dynamics, with a percentage difference of 2% during systole phase and 13% during the diastole. The percentage of blood volume in the CFD simulation with a shear stress above the threshold of 50 Pa is less than 0.001%. In conclusion, the application of this workflow to the Carmat-TAH provided consistent results with previous clinical studies demonstrating its utility in calculating local hemodynamic quantities in the presence of complex moving boundaries. **Key Words:** Fluid–structure interaction—Computational Fluid dynamics—Blood damage evaluation—Total Artificial Heart—Carmat.

Heart failure is a progressive and often fatal pathology among the main causes of death in the world. The treatment of this pathology is generally palliative, which includes drugs, cardiovascular rehabilitation, and multi-site pacing. The only effective long-term treatment for patients with advanced bi-ventricular heart failure is whole heart transplantation, which is associated with the problem of the chronic shortage of donors hearts (1). An alternative to heart transplantation is a totally implantable artificial heart (TAH). The development of mechanical circulatory support systems, the history of the artificial heart, and the role and significance of existing TAH technologies can be found in the literature (2–6).

Although the hemocompatibility of an artificial ventricle depends on the materials used at the blood interfaces, the quantification of the hemodynamics is also important as it can lead to blood damage. Blood damage includes different mechanisms such as hemolysis, platelet activation, destruction of the von Willebrand factor (vWf), alteration of the coagulation cascade, thrombosis and emboli, and reduced functionality of the white blood cells (7). Hemolysis, which is the destruction of red blood cells due to

doi: 10.1111/aor.13316

Received October 2017; Revised April 2018; Accepted June 2018

Address correspondence and reprint requests to Francesco Migliavacca, PhD, Laboratory of Biological Structure Mechanics (LaBS), Department of Chemistry, Materials and Chemical Engineering "Giulio Natta", Politecnico di Milano, Milan, Italy. E-mail: francesco.migliavacca@polimi.it

membrane breakage, is caused by high shear stress (typically above 150 Pa) with a sufficient exposure time (typically above 100 ms) (8). The activation of platelets, cells without a nucleus involved in physiological hemostasis and pathological thrombosis, is also caused by mechanical shearing associated with the exposure time (typically above 50 ms) (8,9). Hemolysis can lead to hemolytic anemia whereas the platelet activation can lead to cerebral stroke after a while. The thrombogenic potential of a blood pumping device, as a matter of fact, can be evaluated by the quantification of the shear stress field (10). Another important aspect that can descend from a nonphysiological shear stress is the conformation change of vWf, which also influences the platelet deposition and aggregation (11–13).

Shear strain rate, defined as the local gradient in velocity between adjacent flow streamlines, is usually calculated from numerical simulations. Gathering accurate values of the shear strain rate and the shear stress will help to estimate the blood damage (14).

Computational fluid dynamics (CFD) and fluid–structure interaction (FSI) models can be employed to investigate the fluid dynamic behavior of the blood, as well as the kinematics of the TAH components, for example, the membrane and the valve leaflets (15).

CFD and FSI approaches are different. CFD calculates the flow field with prescribed pressures and/or flow rates at the inlets/outlets of a model. The model usually has rigid or moving walls, whose displacements are a boundary condition set. FSI evaluates the fluid dynamics and the structure displacements as results of inlet/outlet pressures or volume flow rates. In other words, in the FSI approach, the results of the structural part directly impact the fluid dynamic fields and vice versa (properly defined two-way FSI).

In the past, different CFD models were adopted to investigate TAHs by imposing moving boundaries to the fluid domain using theoretical (16) and experimental data (17). The membrane motion was prescribed in those studies, which, however, did not include biological valves. Marom et al. (10) studied the influence of the presence of disk valves in a TAHs model by imposing a theoretical movement and describing the membrane movement with a mathematical function. Avrahami et al. (18) compared a CFD analysis based on the experimental wall movement with a fully coupled FSI simulation; these authors concluded that CFD might be used to accurately describe the behavior of a ventricular assist device. However, in their study, the valve leaflets were modeled in fully open or fully closed positions both in the CFD and FSI models. A number of researchers used 3D FSI analyses considering the interaction between the membrane and the fluids, but neglecting the valve opening and closing movements at each inlet/outlet surfaces during the cardiac cycle (19–21). Others studies considered the disk valve motion but only in a 2D model (22). The FSI studies, like the one described by Avrahami et al. (18), adopted an arbitrary Lagrangian–Eulerian (ALE) kinematic approach, with a moving fluid grid according to the structure displacement; it reproduced accurately the hemodynamics near the structures, to estimate for example the blood damage indexes like wall shear stress and particle residence time (23). It is also known that the ALE formulation guarantees very accurate results near the interface between the solid structures and the fluid (24) with respect to the fixed grid approaches, for example, the immersed boundary method, which is an alternative relatively less computationally expensive than the FSI approach. In fact, numerical FSI simulations with ALE method and the inclusion of deformable valves are computationally expensive due to the necessary remeshing step. Furthermore, these simulations need particular attention to ensure the continuity of the fluid domain during the diastole, when the valves are closed and any fluid gap is absent (25). To the best of the authors' knowledge, literature works with an ALE description of an artificial ventricle with biological valves are missing. To best of our knowledge, the FSI studies of TAH in the literature (18–23) consider only mechanical valves.

The aim of this work is to provide a robust computational workflow suitable to the study of the membrane, the valve and the fluid dynamics within an existing artificial ventricle, namely the left chamber of the Carmat-TAH. To this purpose, an FSI simulation based on a non-boundary fitted method is proposed followed by a detailed CFD simulation, which allows a better capture of the local hemodynamic quantities, like the shear rate, hardly feasible with the FSI. A CFD simulation with the calculated membrane movement, but neglecting the valve dynamics, is also included to show the important impact of the presence of the valves on the fluid dynamics within the chamber.

MATERIALS AND METHODS

The Carmat-TAH (Fig. 1a) is a bioprosthetic pulsatile electro-hydraulic biventricular support to replace the heart in patients with end-stage heart failure. It works under a pulsatile flow, mimicking the natural heart with an adaptive flow according to the patient needs (1). It is composed of two ventricles

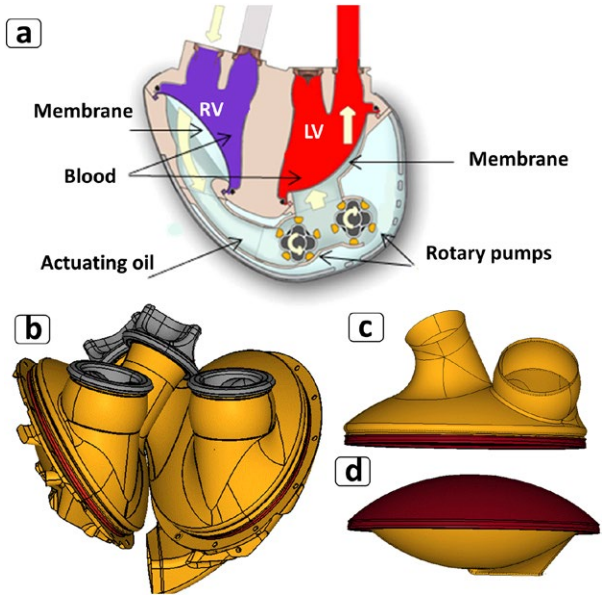

FIG. 1. (a) Carmat total artificial heart with left (LV) and right ventricles (RV) (26), (b) CAD model of the both ventricles, (c) blood wall, (d) membrane (in red) and oil wall of the left ventricle. [Color figure can be viewed at wileyonlinelibrary.com]

containing a hydraulic fluid (silicone oil) and a blood cavity separated by a flexible hybrid membrane composed of two layers, polyurethane in contact with the hydraulic fluid and pericardium in contact with the blood. Two electric rotary pumps reproducing a physiological systolic and diastolic phase actuate the silicone oil part of the circuit (1). A polyurethane sac around the TAH containing the hydraulic fluid reserve works as a compliance chamber. Electronic sensors and microprocessors embedded into the Carmat-TAH automatically adjust the beat rate (up to 161 bpm) and the stroke volume (up to 60 mL) according to the venous return to produce a pulsatile blood flow. Ultrasound transducers, placed inside the oil cavity, detect the position of the membrane. A grid of small hemispheric pattern is placed at the center of the polyurethane layer to improve the echogenicity.

FSI simulation

The geometry of the left chamber, extracted from the entire CAD model of the entire Carmat-TAH, is shown in Fig. 1b. It is composed of the oil compartment, the membrane and the blood compartment (Fig. 1c and d). The volume of the left and right chambers of the Carmat-TAH are 50 and 30 cc, respectively. The valves are 16-mm height with a diameter of 25 mm. The internal surfaces of the original model were considered for the oil and blood walls. Blood and oil walls do not change shape during the functioning; thus, they can be modeled as rigid bodies. All parts were discretized with Hypermesh (Altair Eng. Inc., Troy, MI, USA). The walls were meshed with 28 718 quadrangular shell elements with a thickness of 0.1 mm (Fig. 2a). The membrane was the main deformed part and it was composed of two different layers: polyurethane on the oil side and pericardium on the blood side (Fig. 2b). The membrane was discretized with 55 958 eight-node hexahedral solid elements by mapped meshing. The walls and the membrane were connected node by node to prevent any leakage of fluid and any artificial contact between the membrane and the walls. The inlet and outlet biological valves were modeled with a thickness of 0.25 mm. After a mapped meshing with 1806 fully integrated four-node quadrangular shell elements (single valve), the valves were placed at the location of the real device (Fig. 2a). The adopted meshes have a number of elements established on the basis of accuracy estimations from previous studies of ours (26,27). The fluid parts were built according to the shape of the walls. Four components were defined: fluid domain, which could be either blood or oil depending on the movement of the membrane, oil inlet, mitral inlet, and aortic inlet (Fig. 2c). The fluid parts, considered as a Newtonian fluid, were meshed with Eulerian hexahedral elements with a high quality of uniform and totally cube-like elements. The element size was about 0.76 mm. The total element number for the fluid domains was 443 134. All TAH materials were considered elastic by fitting experimental data provided by Carmat (data not shown). The properties assigned to the different model parts are listed in Table 1.

The rigid walls and the edges of the membrane and the leaflets in contact with the wall were fixed in all directions. The outer surface of the fluid domain was fixed in all directions. The simulations consisted of two steps: (i) a pressurization step ("P" in Fig. 3) where the pressure in the aorta inlet started from zero and reached the physiological value of 120 mm Hg, while the pressure at the mitral inlet was kept to zero; these pressure values were kept constant for the rest of the simulation; (ii) a volume flow rate curve was imposed on the oil inlet to reproduce two cardiac cycles (Fig. 3). The imposed volume flow rate provided a 60 mL of stroke volume, with a frequency of 90 bpm and 33% systole/cycle time ratio according to the standard working condition of the Carmat-TAH. Three couplings were set up to simulate the FSI during the cardiac cycles: (i) between the fluid and the rigid wall, (ii) between the fluid and the valves, and (iii) between the fluid and the membrane. More details about the FSI method can be found in

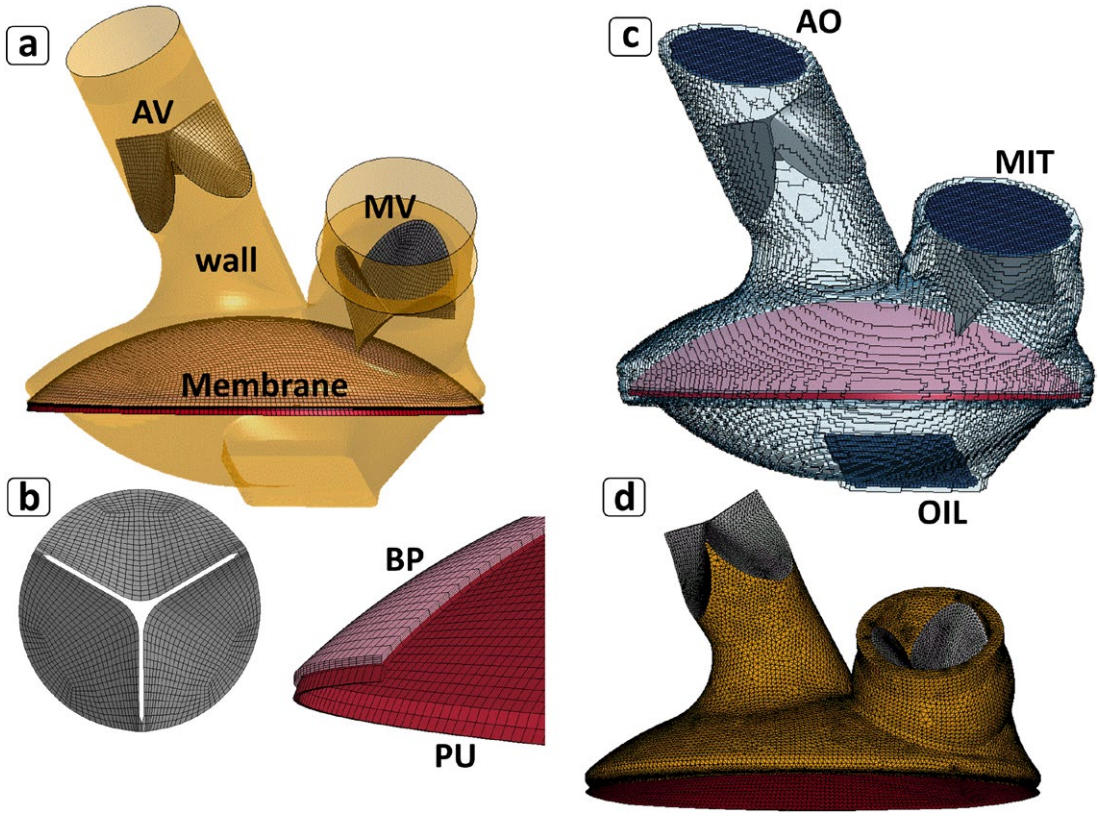

FIG. 2. (a) Left ventricle rigid wall (yellow) with the meshed membrane inside, the aortic valve (AV) and the mitral valve (MV); (b) mesh details of the valve and the membrane composed of bovine pericardium (BP) on the blood side and polyurethane (PU) on the oil side; (c) fluid mesh, where the structures are immersed in, with oil (OIL), mitral (MIT) and aortic (AO) inlets; (d) CFD mesh of the blood domain between the membrane and the valves. [Color figure can be viewed at wileyonlinelibrary.com]

TABLE 1. *Material properties of the different model components*

	Density (g/cm^3)	Elastic modulus (MPa)	Poisson ratio	Viscosity ($Pa \bullet s$)
Polyurethane	1.1	14	0.4	—
Pericardium	1.1	3.2	0.4	—
Walls	1.3	3500	0.4	—
Valves	1.1	8	0.48	—
Blood	1.06	—	—	0.00356
Oil	0.96	—	—	0.0249

previous studies of ours (26,27). FSI simulations were performed with LS-DYNA 971 Release 9.0 (LSTC, Livermore CA, USA). Results are displayed at representative time points of the cardiac cycle: 0.76 s (t_0), 0.82 s (t_1), 0.94 s (t_2), 1.12 s (t_3), 1.25 s (t_4), and 1.38 s (t_5) (Fig. 3). They correspond to the starting point of the cardiac cycle (t_0), the evolution of the diastole (from t_1 to t_3) and the evolution of the systole (from t_4 to t_5).

CFD investigation

The mesh of the CFD model was created considering the blood between the membrane and the two valves. The CFD meshes (Fig. 2d) are composed of 970 285 tetrahedral elements. Fluent 18.0 (ANSYS Inc., Canonsburg, PA, USA) was used for the computations. A user-defined function was used to prescribe the membrane and the valves displacements at each time-step as obtained from the FSI analysis. The implemented algorithm is based on the coupling of the nodes belonging to the fluid domain face in the CFD model with those belonging to the structural domain of the FSI model. For comparison, a simplified model in which the valves were replaced with inlet and outlet surfaces was also considered.

Blood shear stress was calculated in the 3D blood domain, inside the ventricle, to quantify blood

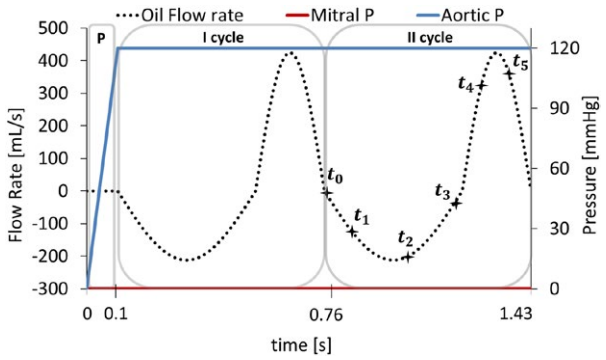

FIG. 3. Imposed oil flow rate (black dotted line), mitral pressure (red line), and aortic pressure (blue line). Black stars on the curve are the time points where results are analyzed. [Color figure can be viewed at wileyonlinelibrary.com]

damage, based on the results of the CFD simulations. Blood damage was evaluated in terms of volumetric distribution of shear stress (28,29) with regard to specified thresholds for hemolysis (150 Pa) and platelets activation (50 Pa) (8).

RESULTS

FSI simulation

The displacement of the membrane and valves, and the Von Mises stresses in the membrane are synthetically shown in Fig. 4. After the pressurization step, the oil and blood pressures were negative and the mitral valve with zero-pressure in the mitral inlet was open. Then the pressure in the blood side increased until exceeding the 120 mm Hg of the aortic outlet and the aortic valve moved to the open configuration. During the heart cycle, the membrane completely unfurled and experienced an inversion in curvature as demonstrated in Fig. 5, which illustrates the membrane's median line at different time points. Figure 6, left column, reports the velocity color maps on a median cross section in five different instants during the cardiac cycle.

CFD investigation

The mid and right columns in Fig. 6 show the velocity contour maps on a median cross section for the two CFD simulations (with and without valves). The maximum velocity values in the left ventricle at the five different instants of the cardiac cycle are also reported. Differences among the models with valves and without valves were remarkable. In fact, the velocities in the CFD simulation with valves, considered as the reference model, were more similar to those evaluated with the FSI model. The percentage difference varied between 2% and 13% in the different instants, whereas it shows greater values (from 4 to 45%) when compared to the results of the CFD

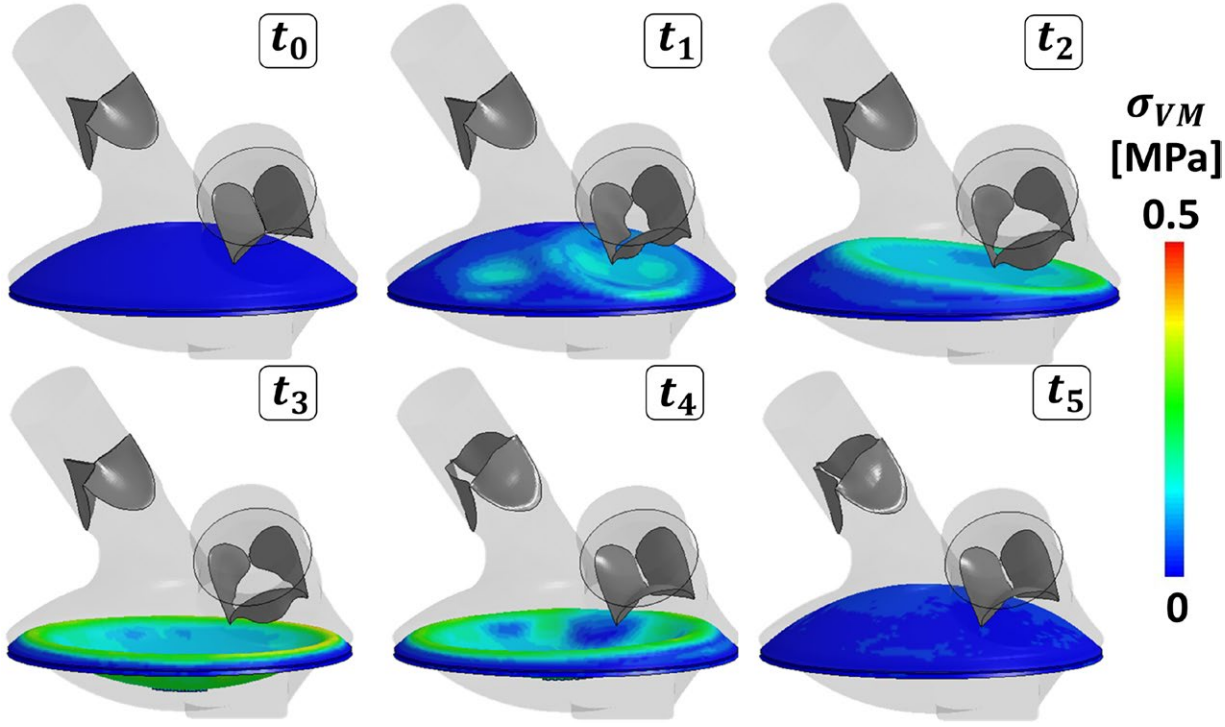

FIG. 4. FSI kinematics of the membrane and the valves, and Von Mises stresses of the membrane in the simulated cycle. [Color figure can be viewed at wileyonlinelibrary.com]

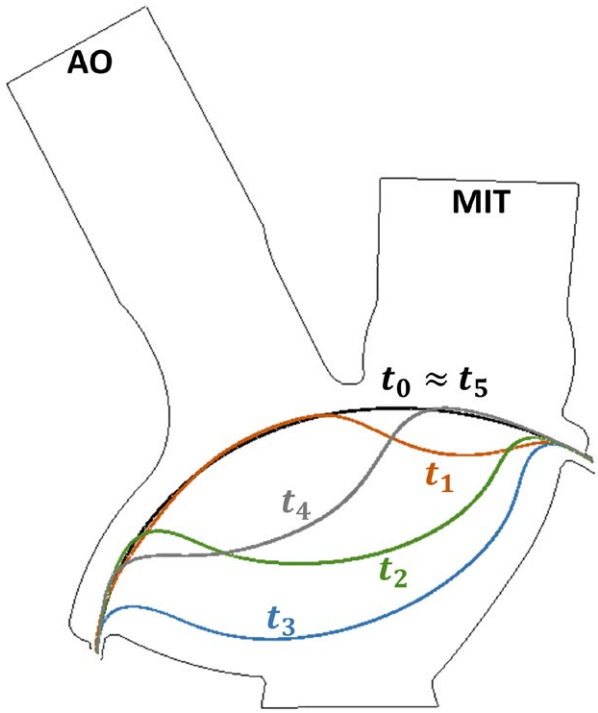

FIG. 5. FSI membrane displacement at different time points during the cardiac cycle. [Color figure can be viewed at wileyonlinelibrary.com]

model without valves. The smallest difference, as expected, was visible when the aortic valve was fully opened (differences between 2 and 4%). This figure clearly shows that incorporating the valve dynamics in the CFD simulations leads to a more realistic representation of the blood hemodynamics in the ventricle, where the typical jet-like structures near the valves are created.

As for blood damage, less than 0.001% of ventricle's blood volume was found according to a shear stress above each threshold. The high shear stress area was located around the aortic valve where the flow was high during the systolic phase (Figs. 6–8). These first results indicate an a priori good hemocompatibility, which was coherent with previous in vivo (30,31) and clinical results (32,33).

DISCUSSION

In this study, a new workflow to reproduce the hemodynamics inside the left chamber of the Carmat-TAH together with the movement of the aortic and mitral valves and the membrane is presented. Although in the recent years numerical studies about the TAH have been conducted, with both FSI and CFD numerical analyses, there are still a significant number of simplifications and limitations, for example, the a priori prescription of the displacement of the (16) or of the valve leaflets (10), the presence of the valves, but only in fixed opening or closing configurations (18–21). To the best of the authors' knowledge, this is the first work where a CFD analysis of a TAH considers the realistic movement of both membrane and valves to evaluate blood damage.

We compared two CFD simulations with moving boundaries (with and without valves) to show that the fluid dynamic field in the absence of the valves (although with the same membrane motion) substantially differs from the one with valves, in terms of both global and local hemodynamics, for example, the shear rate field and velocity fields with jet-like shape. The CFD simulation without valves is a distinctive feature of biological valves, as reported in some experimental tests (34,35).

In the literature, to the best of the authors' knowledge, biological valves have not been considered when simulating an artificial ventricle. There are, however, a few CFD studies with mechanical valves (18–23), whose leaflets move as rigid bodies under a prescribed roto-translational displacement in the CFD simulations.

The quantification of blood damage is important when analyzing the behavior of an artificial ventricle. The in silico hemolysis prediction is based on a reliable description of the blood fluid dynamics inside the device (15). For this reason, the fluid domain needs to be numerically described with an ALE kinematic approach (36), which rises the issue of modeling the valves in TAH devices. Mechanical valves can be studied with an ALE approach to ensure the continuity of the fluid domain upstream and downstream from the valves (10,22); while the modeling of biological or deformable valves is much more difficult (25). This work proposes a robust simulation methodology to evaluate the hemodynamics of the left chamber of the Carmat-TAH. Firstly, an FSI simulation was carried out. From the original CAD files, the geometry of the external wall, the membrane and the two biological valves were obtained; after the discretization phase, all the structures were immersed in a fluid grid in order to obtain a complete and realistic simulation that took into account the coupling between the membrane and the valves with the fluids in the ventricle. Mesh sensitivity tests were performed for the structural and fluid grids based on the experience of previous studies (26,27). The boundary conditions prescribed to the model were chosen with the aim to reproduce a physiological working environment. The imposition of different boundary conditions in terms of heart rate or aortic pressure is a future step

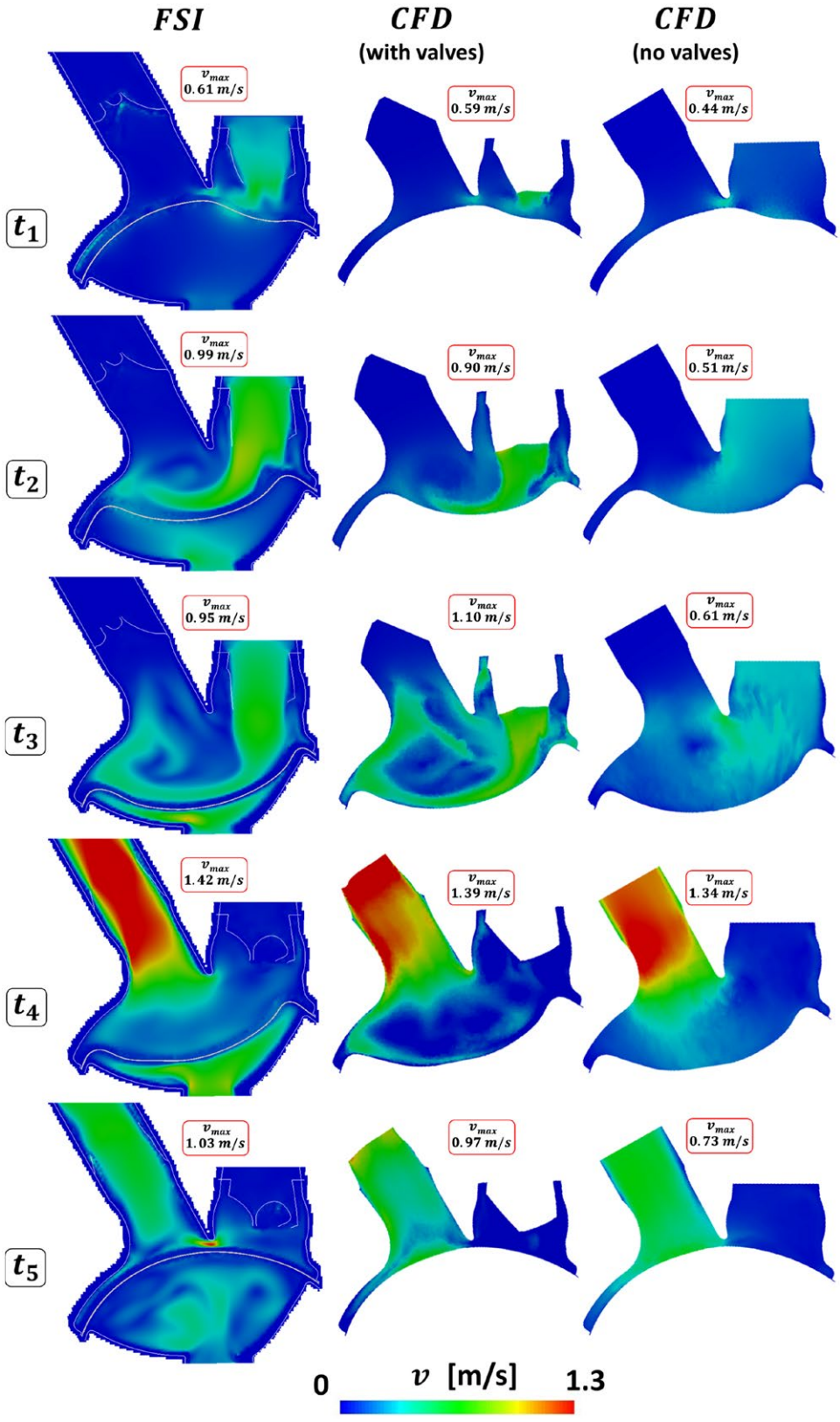

FIG. 6. Comparison of velocity fields from FSI, CFD-with valve and CFD-without valve at different time points along the cardiac cycle. The maximum velocities in the entire blood domain are reported. [Colour figure can be viewed at wileyonlinelibrary.com]

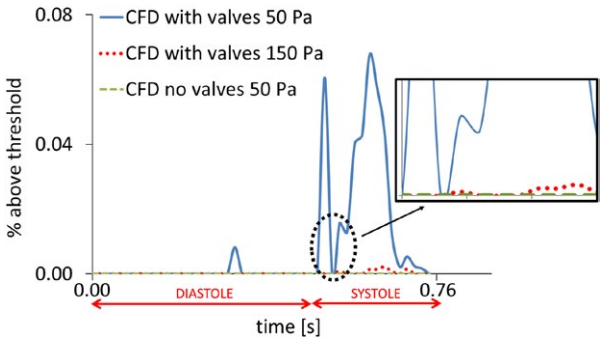

FIG. 7. Percentage of the blood inside ventricular cavity subjected to a shear stress above 50 Pa and 150 Pa during one cardiac cycle. The inset shows the curves when the aortic valve is opening. [Color figure can be viewed at wileyonlinelibrary.com]

to better investigate the effects of these parameters on the global and the local hemodynamics.

In the second part of the work, as the fixed grid approach does not resolve the immersed surfaces accurately (25), the blood domain was analyzed with a CFD simulation imposing the structure movement (membrane and valves) as resulted from the FSI simulations. In particular, the presence of the valves was assessed in the CFD simulations. The comparison between FSI and CFD velocity fields confirmed that the presence of the valves in the CFD model is important to reproduce realistic blood dynamics. The adopted workflow composed of sequential simulations can obtain accurate fluid dynamic features, hardly caught by a sole FSI analysis based on a fixed grid technique. Since, wall shear stresses, vortices, and local vector velocity fields nearby the interface between solid structures and fluid in the FSI simulations are not reliable the proposed workflow can easily be applied to evaluate indexes as the ratio of blood subjected to high shear stress at each time-step.

In addition, a comparison of the hemocompatibility performance between several geometries during preclinical studies can also be made (30,31), thus optimizing hemocompatibility design. Some recent works (12,36–38) adopted the shear stresses as the main parameter to evaluate blood damage indexes in VAD or TAH devices, stressing the importance to obtain reliable fluid dynamic results from the numerical simulations. They used these indexes of their hydrodynamic performance and hemodynamic characteristics to analyze, compare, or evaluate different devices. Nascimbene et al. (12) proved the strictly relation between shear stress and hemolysis. Recent works (36,37) on VADs showed a relative fluid volume with shear stress above the threshold of 150 Pa comparable with our results. Moreover, in the validation work of Wappenschmidt et al. (36), the goodness of the FSI methodology to calculate this hemolysis indexes was verified. In vivo analysis in calves confirmed that the Carmat-TAH maintains the hemodynamic parameters in an acceptable range (30) with no signs of coagulation activation (31). In this regard, results from our simulations with less than 0.001% of ventricle's blood volume with a shear stress above the threshold is consistent with these experimental observations indicating the soundness and potentialities of the proposed workflow.

This study has limitations. First is the assumption of constant pressure on the mitral inlet and aortic outlet. The autoregulation of these pressures was not incorporated into the model and needs to be addressed in future works by introducing a lumped parameter boundary condition. This could reproduce the real capability of a TAH to adapt the working conditions to the patient's needs. Second, due to the long computational time, only two cardiac cycles were reproduced

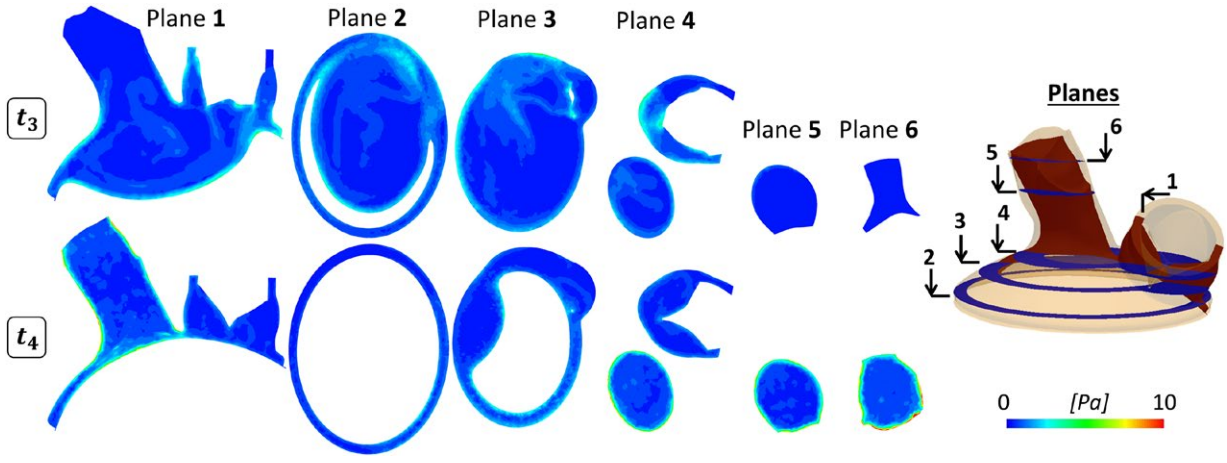

FIG. 8. Shear stress contour maps in diastole ($t = t_3$) and systole ($t = t_4$) plotted in six different planes. [Color figure can be viewed at wileyonlinelibrary.com]

in the CFD analysis; a more focused investigation on the remeshing algorithm could resolve this problem and allow performing washout studies. An additional future development of this work is to perform an experimental test to validate this sequential approach. However, by analyzing the valve leaflet motion, we observed a behavior similar to that examined in previous studies of ours (26,27) and by other groups (39,40), who compared the numerical results with experimental evidence. Although we do not have specific experimental data to validate the prediction of the membrane motion, we believe that our results can be representative of a realistic behavior.

CONCLUSION

The numerical workflow presented in this work describes the local hemodynamics in an artificial ventricle with fairly good reliability. The shear rate values and the local hemodynamics can be used for the estimation of blood damage in total artificial heart devices. The application to the Carmat-TAH provides consistent results with those from previous clinical studies and demonstrate the relevance of the workflow. The comparison of the hemocompatibility performances across different designs during preclinical investigations would offer the capability to optimize the geometry and to better predict hemodynamic aspects for future TAH or VAD developments.

Acknowledgment: The authors thank Monique Lopez for thoroughly editing the manuscript.

Author contributions: GL and WW designed the study, implemented and tested the computational framework, and drafted the manuscript. HDC supported the implementation of the study, performed the data analysis and revised the manuscript. FM, JFRM, GD, MG, and PD conceived the study, participated in its design and coordination, and helped to draft and revise the manuscript. All the authors read and approved the final manuscript.

Conflicts of Interest: The authors have declared no conflicts of interest for this article.

REFERENCES

1. Mohacsi P, Leprince P. The CARMAT total artificial heart. *Eur J Cardio-Thoracic Surg* 2014;46:933–4.
2. Copeland JG, Smith RG, Arabia FA, et al. Cardiac replacement with a total artificial heart as a bridge to transplantation. *N Engl J Med* 2004;351:859–67.
3. Cook JA, Shah KB, Quader MA, et al. The total artificial heart. *J Thorac Dis* 2015;7:2172–80.
4. Pelletier B, Spiliopoulos S, Finocchiaro T, et al. System overview of the fully implantable destination therapy—ReinHeart-total artificial heart. *Eur J Cardio-Thoracic Surg* 2015;47:80–6.
5. Cohn WE, Timms DL, Frazier OH. Total artificial hearts: past, present and future. *Nat Rev Cardiol* 2015;12:609–17.
6. Petukhov DS, Selishchev SV, Telyshev DV. Total artificial heart: state-of-the-art. *Biomed Eng (NY)* 2015;49:193–6.
7. Fraser KH, Zhang T, Taskin ME, Griffith BP, Wu ZJ. A quantitative comparison of mechanical blood damage parameters in rotary ventricular assist devices: shear stress, exposure time and hemolysis index. *J Biomech Eng* 2012;134:81002.
8. Alemu Y, Bluestein D. Flow-induced platelet activation and damage accumulation in a mechanical heart valve: numerical studies. *Artif Organs* 2007;31:677–88.
9. Stassen JM, Arnout J, Deckmyn H. The hemostatic system. *Curr Med Chem* 2004;11:2245–60.
10. Marom G, Chiu W-C, Crosby JR, et al. Numerical model of full-cardiac cycle hemodynamics in a total artificial heart and the effect of its size on platelet activation. *J Cardiovasc Transl Res* 2014;7:788–96.
11. Di Stasio E, De Cristofaro R. The effect of shear stress on protein conformation: physical forces operating on biochemical systems: the case of von Willebrand factor. *Biophys Chem* 2010;153:1–8.
12. Nascimbene A, Neelamegham S, Frazier OH, Moake JL, Dong J-F. Acquired von Willebrand syndrome associated with left ventricular assist device. *Blood* 2016;127:3133–41.
13. Chen Z, Mondal NK, Ding J, Koenig SC, Slaughter MS, Wu ZJ. Paradoxical effect of nonphysiological shear stress on platelets and von Willebrand factor. *Artif Organs* 2016;40:659–68.
14. Foin N, Gutiérrez-Chico JL, Nakatani S, et al. Incomplete stent apposition causes high shear flow disturbances and delay in neointimal coverage as a function of strut to wall detachment distance: implications for the management of incomplete stent apposition. *Circ Cardiovasc Interv* 2014;7:180–9. American Heart Association, Inc.
15. Fraser KH, Taskin ME, Griffith BP, Wu ZJ. The use of computational fluid dynamics in the development of ventricular assist devices. *Med Eng Phys*. 2011;33:263–80.
16. Kiris C, Kwak D, Rogers S, Chang ID. Computational approach for probing the flow through artificial heart devices. *ASME* 1997;119:452–60.
17. König CS, Clark C, Mokhtarzadeh-Dehghan MR. Investigation of unsteady flow in a model of a ventricular assist device by numerical modelling and comparison with experiment. *Med Eng Phys* 1999;21:53–64.
18. Avrahami I, Rosenfeld M, Raz S, Einav S. A numerical model of flow in a sac—type ventricular assist device. *Artif Organs* 2006;30:529–38.
19. Bazilevs Y, Long CC, Marsden AL. Fluid-structure interaction simulation of pulsatile ventricular assist devices. *Comput Mech* 2013;52:971–81.
20. Yang XL, Liu Y, Yang JM. Unsteady flow and diaphragm motion in total artificial heart. *J Mech Sci Technol* 2007;21:1869–75.
21. Sonntag SJ, Kaufmann TAS, Büsen MR, et al. Simulation of a pulsatile total artificial heart: development of a partitioned Fluid Structure Interaction model. *J Fluids Struct* 2013;38:187–204.
22. Moosavi MH, Fatouraee N. Flow Simulation of a Diaphragm-type Ventricular Assist Device with Structural Interactions. 2007 29th Annu Int Conf IEEE Eng Med Biol Soc. *IEEE*;2007:1027–30.

23. Sonntag SJ, Kaufmann TAS, Büsen MR, et al. Numerical washout study of a pulsatile total artificial heart. *Int J Artif Organs* 2014;37:241–52.
24. Wall WA, Gerstenberger A, Gamnitzer P, Förster C, RammE. Deformation fluid-structure interaction—advances in ale methods and new fixed grid approaches. *Fluid-Structure Interact* 2006;195–232.
25. Bavo AM, Rocatello G, Iannaccone F, Degroote J, Vierendeels J, Segers P. Fluid-structure interaction simulation of prosthetic aortic valves: comparison between immersed boundary and arbitrary Lagrangian-Eulerian techniques for the mesh representation. *PloS One*. 2016;11:e0154517.
26. Luraghi G, Wu W, De Gaetano F, et al. Evaluation of an aortic valve prosthesis: fluid-structure interaction or structural simulation? *J Biomech* 2017;58:45–51.
27. Wu W, Pott D, Mazza B, et al. Fluid-structure interaction model of a percutaneous aortic valve: comparison with an in vitro test and feasibility study in a patient-specific case. *Ann Biomed Eng* 2016;44:590–603.
28. Chua LP, Su B, Lim TM, Zhou T. Numerical simulation of an axial blood pump. *Artif Organs* 2007;31:560–70.
29. Thamsen B, Blümel B, Schaller J, et al. Numerical analysis of blood damage potential of the HeartMate II and HeartWare HVAD rotary blood pumps. *Artif Organs* 2015;39:651–9.
30. Latrémouille C, Duveau D, Cholley B, et al. Animal studies with the Carmat bioprosthetic total artificial heart. *Eur J Cardio-Thoracic Surg* 2015;47:e172–9.
31. Smadja DM, Susen S, Rauch A, et al. The Carmat bioprosthetic total artificial heart is associated with early hemostatic recovery and no acquired von Willebrand syndrome in calves. *J Cardiothorac Vasc Anesth* 2017;31:1595–602.
32. Carpentier A, Latrémouille C, Cholley B, et al. First clinical use of a bioprosthetic total artificial heart: report of two cases. *Lancet* 2015;386:1556–63.
33. Smadja DM, Saubaméa B, Susen S, et al. Bioprosthetic total artificial heart induces a profile of acquired hemocompatibility with membranes recellularization. *J Am Coll Cardiol* 2017;70:404–6.
34. Leo HL, Dasi LP, Carberry J, Simon HA, Yoganathan AP. Fluid dynamic assessment of three polymeric heart valves using particle image velocimetry. *Ann Biomed Eng* 2006;34:936–52.
35. Hasler D, Landolt A, Obrist D. Tomographic PIV behind a prosthetic heart valve. *Exp Fluids* 2016;57:80.
36. Wappenschmidt J, Sonntag SJ, Buesen M, et al. Fluid dynamics in rotary piston blood pumps. *Ann Biomed Eng* 2017;45:554–66.
37. Wiegmann L, Bo SS, De Zé Licourt et al. Blood pump design variations and their influence on hydraulic performance and indicators of hemocompatibility. *Ann Biomed Eng.* 2017;46:417–28.
38. Chen Z, Jena SK, Giridharan GA, et al. Flow features and device-induced blood trauma in CF-VADs under a pulsatile blood flow condition: a CFD comparative study. *Int J Numer Method Biomed Eng* 2018;34:e2924.
39. Sigüenza J, Pott D, Mendez S, et al. Fluid-structure interaction of a pulsatile flow with an aortic valve model: a combined experimental and numerical study. *Int J Numer Method Biomed Eng* 2018;e2945.
40. Gharaie SH, Mosadegh B, Morsi Y. In vitro validation of a numerical simulation of leaflet kinematics in a polymeric aortic valve under physiological conditions. *Cardiovasc Eng Technol* 2018;9:42–52.